

Homogeneous buffer layer technique for the growth of Al doped ZnO films on flexible substrate

JIANFENG SU*, CHUNHE ZANG, QIANG NIU, RUIRUI SUN, JIAO ZHANG, YONGSHENG ZHANG

Department of mathematics and Physics, Luoyang institute of science and technology, Luoyang 471023, China

Al doped ZnO films were grown on PI flexible substrate by Sol-Gel method. To improve the optical and electrical properties, homogeneous buffer layers were introduced before the grown of ZnO films using magnetron sputtering technology. A systematical and detailed study of the effect of buffer layer sputtering time on structural, optical and electrical properties were discussed using XRD, SEM and PL. For samples with homogeneous buffer layer, excellent crystallization quality and optical properties were obtained. Moreover, as increasing the sputtering time of buffer layer, the properties of ZnO films were improved further. All Al-doped samples demonstrate more than 85% of the optical transparency in the visible region. Low electrical resistivity of Al-doped ZnO films was obtained. However, as the increased of buffer layer sputtering time, due to defects and grain boundary scattering which caused by thicker buffer layer, the hall mobility is increased initially and then decreased.

(Received August 4, 2016; accepted June 7, 2017)

Keywords: ZnO, Flexible substrate, Al doped, Buffer layer

1. Introduction

Recently, ZnO:Al (AZO) as n-type TCO thin films are intensively researched to replace ITO thin films, because they are non-toxic and cost-effective [1]. Furthermore, AZO shows comparable electrical and optical properties with that of ITO [2]. On the other hand, the preparation of TCO on organic substrates becomes more and more important for the use in flexible device technique such as flexible solar cells, flexible displays, flexible OLEDs and so on [3,4]. Generally, the AZO thin films with low resistivity and high transmittance in the visible region are usually grown under temperature higher than 200 °C [5,6]. Unfortunately, such a high temperature always prohibits AZO films from being deposited on polymer substrates, which limits AZO's applications in flexible devices. Up to now, compared with the other deposition techniques, sol-gel has been recognized as the most efficient methods to obtain transparent and conductive ZnO based films at lower temperature with excellent compositional control, homogeneity on the molecular level due to the mixing of liquid precursors [7,8]. So, in our work, sol-gel method was adopted to synthesis ZnO:Al TCO thin films. However, the thin films grown by sol-gel method on flexible substrates are easily peeling off from the substrate. Accord to P. Bertrand's reports that the ion bombardment causes surface damages with bond breaking and it results a highly activated surface which will improve the adhesion [9]. Therefore, we are motivated to pretreat the flexible substrates by Ar ion bombardment technology. While, the

properties of AZO thin films which were grown directly on substrates with Ar ion bombardment is not satisfactory. So it is necessary to find another method to improve the quality of AZO thin films. A common method to solve this problem is to employ buffer layer technology [10,11]. And according to Pei and Carvalho's reports, the buffer layer technology can effectively reduce the resistivity of conductive films [12,13]. Therefore, in this paper, homogeneous buffer layers were introduced before the grown of ZnO films using magnetron sputtering technology. A systematical and detailed study of the effect of buffer layer sputtering time on structural, optical and electrical properties were discussed.

2. Experimental procedure

The ZnO:Al thin films were grown using the aqueous sol prepared by zinc acetate dehydrate, aluminium chloride and polyvinyl alcohol (PVA). The concentrations of Zn^{2+} and Al^{3+} were 0.6 mol/l. Before the deposition of ZnO buffer layer, the cleaned PI flexible substrates have been bombarded by Ar^+ plasma. Then the ZnO buffer layers were deposited using RF magnetron sputtering technology. The RF power is 25W, substrate temperature is 150 °C. To vary the thickness of buffer layer, sputtering time is varied from 0 min to 15 min. Then the ZnO:Al films were prepared by sol-gel process. The prepared sol was spin coated on the substrates with ZnO buffer layer and dried at 120 °C in a tubular furnace in air. This process was

repeated six times for each sample. The obtained films were heated at 350 °C for 30 min in a tubular furnace in nitrogen atmosphere. The detailed experimental conditions for ZnO buffer layer are shown in Table 1.

Table 1. Growth parameters for ZnO buffer layer

Sample	RF power(W)	Temp(°C)	Time(min)
S1	25	150	0
S2	25	150	5
S3	25	150	10
S4	25	150	15

Crystallinity of obtained films was analyzed by X-ray diffraction (XRD) using a D-MAX/ γ A system with $\text{CuK}\alpha$ radiation $\lambda=0.154178\text{nm}$ in the range of $30^\circ\sim 80^\circ$. Surface morphologies of ZnO:Al films were observed by a model JEOL-JSM-6700F field emission scanning electron microscope (FESEM). Room temperature photo-luminescence (PL) spectra of samples were measured by a LABRAM-HR Confocal Laser Micro-Raman spectrometer with 325 nm He-Cd laser as an excitation source. Hall-effect measurements were carried out in the van der Pauw configuration at room temperature. A spectrophotometer was used for the measurements of transmittance in the wavelength range of 300 -700 nm.

3. Results and discussion

3.1. Structure and morphology

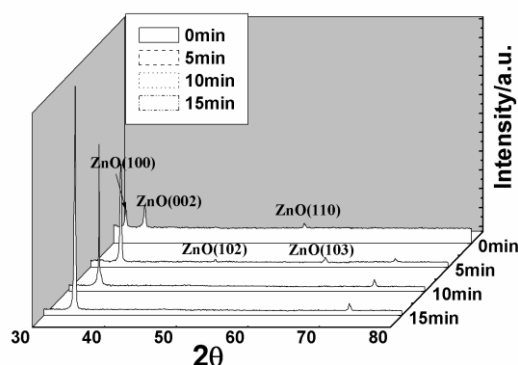


Fig. 1. XRD patterns of ZnO:Al films with different sputtering time for buffer layer. (a) 0min; (b) 5min; (c) 10min; (d) 15min

XRD patterns of ZnO:Al films grown with different sputtering time for buffer layer were shown in Fig. 1. In

the figures, ZnO(002) peaks are observed at around 34.4° in every sample, which indicated that the ZnO:Al films exhibited a strong c-axis preferred orientation and revealed the wurtzite structure. For sample S1, in addition to ZnO (002) diffraction peak, there are two other peaks corresponding to ZnO (100) and (110) planes can be observed. For sample S2, with ZnO buffer layer, the intensity of ZnO (002) diffraction peak strengthened and the ZnO (100) and (110) diffraction peak disappeared. While, another two very weak diffraction peaks which corresponding to ZnO (102) and (103) planes were observed. As increasing the sputtering time of buffer layer further, ZnO (102) and (103) diffraction peaks disappeared, the intensity of ZnO (002) diffraction peak exhibits a remarkable enhancement and the second diffraction peak is also observed. This phenomenon indicated that the ZnO buffer layer undergoes an obvious crystallization improvement at this stage and the crystallinity of ZnO:Al film is significantly improved as increasing the sputtering time of ZnO buffer layer further. It is known that the surface atoms and molecules of amorphous PI substrates arrange randomly. And this surface structure does not conducive to the ZnO thin film grown along the c-axis preferred orientation. When buffer layer was introduced, the influence of the substrate surface defect on ZnO:Al film can be reduced effectively. Then many defects in films will be avoided and fine ZnO:Al films will be obtained.

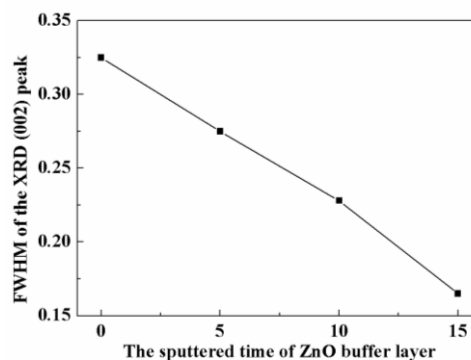


Fig. 2. FWHM of ZnO (002) peak with different sputtering time for buffer layer

Fig. 2 displays the variation of the full width at half maximum (FWHM) of ZnO (002) peak along with the buffer layer sputtered at different time. According to the Scherrer's equation

$$D = \frac{\kappa\lambda}{\Delta(2\theta) \cos \theta} \quad (1)$$

the grain size was calculated, $\kappa=0.89$, $\lambda=0.154$ nm, θ is the (002) diffraction peak of ZnO and $\Delta(2\theta)$ is the FWHM of the (002) peak. The results were 5.11 nm, 20.6 nm, 72.8

nm and 255.6 nm respectively. In addition, no other phases such as metallic zinc or aluminum or Al_2O_3 were detected for all samples.

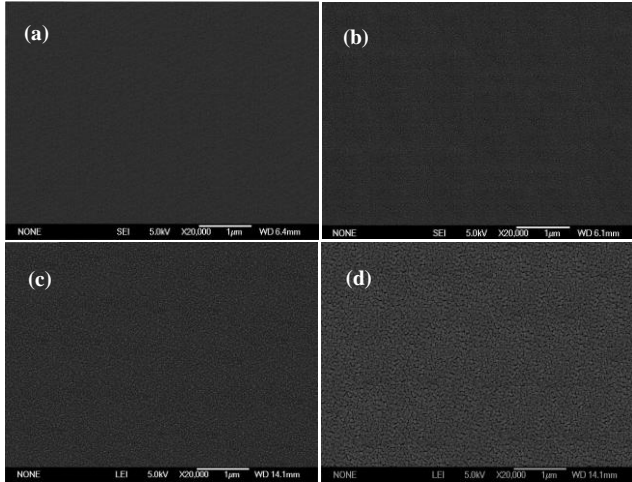


Fig. 3. SEM images of ZnO:Al films with different sputtering time for buffer layer. (a) 0min; (b) 5min; (c) 10min; (d) 15min

In order to illustrate the surface morphology of the ZnO:Al films, SEM images were shown in Fig. 3. It can be seen that, as introducing ZnO buffer layer, the grain size of ZnO increased obviously, and the granule is uniform. This is because that the buffer layer technique improves the matching between substrate and film, thereby benefit to the growth of ZnO:Al films. It is consistent with the XRD results.

3.2. Optical properties

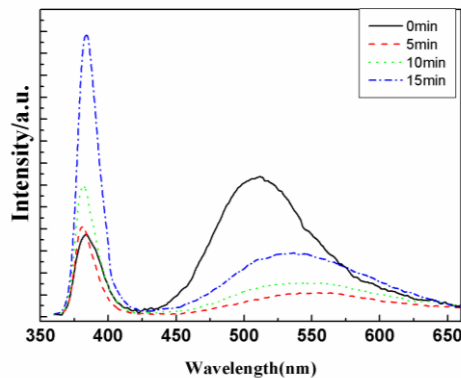


Fig. 4. PL spectra of ZnO:Al films with different sputtering time for buffer layer. (a) 0min; (b) 5min; (c) 10min; (d) 15min

Room temperature PL spectra of ZnO:Al films were also investigated. The PL spectra of ZnO:Al films deposited at various parameters were displayed in Fig. 4. As shown in the figure, when ZnO buffer layer was

introduced, the intensity of the UV emission peak increased while that of the visible emission peak decreased. Normally, the UV emission is attributed to an exciton transition and the visible bands are attributed to deep-level defects in ZnO, such as vacancies and interstitials of zinc and oxygen [14, 15]. The enhancement of the UV peak and the weaken of the visible peak indicated that the crystal quality of ZnO:Al films was improved effectively by ZnO buffer layer technique. This was consistent with the XRD results.

The transmission spectrum in the wavelength range of 300-700 nm for ZnO:Al thin films is given in Fig. 5. It can be seen that for ZnO:Al film without buffer layer the average transmittance in visible region (400-700 nm) was only 70%. As buffer layer was introduced, the average transmittance of ZnO:Al films in visible region increased significantly, and when the sputtering time for buffer layer was increased to 10min, the average transmittance of ZnO:Al films in visible region reached around 85%.

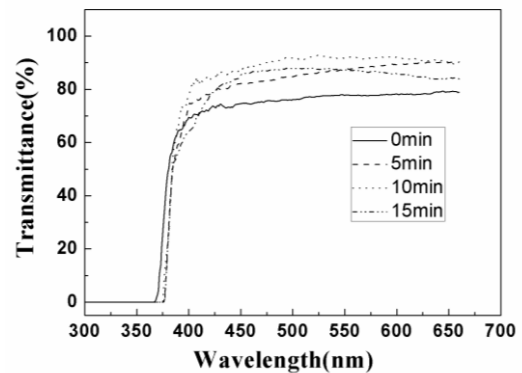


Fig. 5. Transmittance spectrum of ZnO:Al films with different sputtering time for buffer layer. (a) 0min; (b) 5min; (c) 10min; (d) 15min

While, as the sputtering time was increased further, the average transmittance in visible region decreased slightly which might be due to the thicker buffer layer. All films exhibited a sharp fundamental absorption edge when the wavelength of incident light was less than 370 nm.

3.3. Electrical properties

The resistivity, carrier concentration and hall mobility of ZnO:Al films, as a function of sputtering time for buffer layer were measured and listed in Table 2. It can be seen that through preliminary deposition of ZnO buffer layer, the electrical performance of ZnO:Al thin film was ameliorated obviously. When the sputtering time for buffer layer increased from 0 min to 10 min, the resistivity was decreased from $6.32 \times 10^{-3} \Omega \cdot \text{cm}$ to $4.31 \times 10^{-4} \Omega \cdot \text{cm}$, the carrier concentration was increased from $2.4 \times 10^{20} \text{ cm}^{-3}$ to $7.2 \times 10^{20} \text{ cm}^{-3}$ and the hall mobility was increased from $4.12 \text{ cm}^2 \text{ V}^{-1} \text{ s}^{-1}$ to $20.13 \text{ cm}^2 \text{ V}^{-1} \text{ s}^{-1}$. According to the results

listed in Table 2, curves about the resistivity, carrier concentration and mobility versus buffer layer sputtered time have been drawn and shown in Fig. 6.

Table 2. Resistivities and hall mobility of ZnO:Al films with different sputtering time(ST) for buffer layer

ST for buffer layer (min)	Resistivity ($\Omega\cdot\text{cm}$)	Carrier concentration (cm^{-3})	Mobility ($\text{cm}^2/\text{V}\cdot\text{s}$)
0	6.32×10^{-3}	2.4×10^{20}	4.12
5	7.17×10^{-4}	5.6×10^{20}	15.56
10	4.31×10^{-4}	7.2×10^{20}	20.13
15	5.0×10^{-4}	6.8×10^{20}	18.34

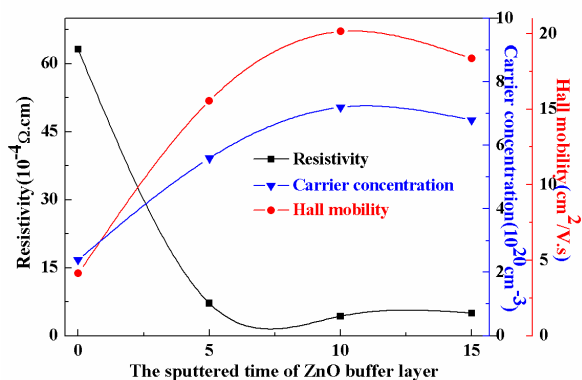


Fig. 6. Electrical properties of ZnO:Al films which contain the resistivity, carrier concentration and Hall mobility with different sputtering time for buffer layer

Generally, the conductivity of film depends on the crystal quality, carrier concentration and hall mobility. Compared with the ZnO:Al films without buffer layer, better crystal quality and more flat surface presented for ZnO:Al films with buffer layer. So the carrier scattering centers inside the film were reduced, the mobility was increased, and better electrical properties was obtained. There was no more improvement for electrical properties when the sputtering time was increased up to 15 min, and even there was a slightly degradation. The reason may be that thicker buffer layer lead to lattice distortion such as defects and grain boundary, and so poorer electrical properties [16].

4. Conclusion

In conclusion, crystal structure, surface morphology, visible transmittance and electrical properties of the

ZnO:Al films coated on PI flexible substrate by ZnO buffer layer technique have been systematically investigated in this study. The results indicate that the sputtering time for buffer layer can significantly affect the properties of the ZnO:Al films. With ZnO buffer layer, all ZnO:Al films oriented with the c-axis perpendicular and had a high transmittance around 85% in visible range. Moreover, the sputtering time of buffer layer had a great effect on electrical properties of the ZnO:Al thin films, especially on the resistivity. As the sputtering time increased, the resistivity decreased while the carrier concentration, the hall mobility and average transmittance increased. The minimum resistivity of $4.31 \times 10^{-4} \Omega\cdot\text{cm}$ combined with highest carrier concentration of $7.2 \times 10^{20} \text{cm}^{-3}$ and highest hall mobility of $20.13 \text{cm}^2\text{V}^{-1}\text{s}^{-1}$ were obtained at 10 min. This high optical transmittance of ZnO:Al thin films could be used in photoelectric devices to meet various requirements.

Acknowledgements

This work was supported by the National Natural Science Foundation of China (Grant Nos. 51302128, 60876041) and the NSF of Henan Province (grant nos.152102210330, 172102210401, 17A430004).

References

- [1] T. Hamaguchi, K. Omae, T. Takebayashi, Y. Kikuchi, N. Yoshioka, Y. Nishiwaki, A. Tanaka, M. Hirata, O. Taguchi, T. Chonan, *Occup. Environ. Med.* **65**(1), 51 (2008).
- [2] H. Kim, J. S. Horwitz, S. B. Qadri, D. B. Chrisey, *Thin Solid Films* **420**, 107 (2002).
- [3] Tingting Guo, Guobo Dong, Fangyuan Gao, Yu Xiao, Qiang Chen, Xungang Diao, *Appl. Surf. Sci.* **282**, 467 (2013).
- [4] Jian Chen, Yihua Sun, Xin Lv, Derong Li, Liang Fang, Hailin Wang, Xiaohua Sun, Caihua Huang, Haizhou Yu, Ping Feng, *Appl. Surf. Sci.* **317**, 1000 (2014).
- [5] A. Suzuki, T. Matsushita, T. Aoki, M. Okuda, *Thin Solid Films* **445**, 263 (2003).
- [6] S. Cornelius, M. Vinnichenko, N. Shevchenko, A. Rogozin, A. Kolitsch, W. Moller, *Appl. Phys. Lett.* **94**, 042103-042103-3 (2009).
- [7] Duy-Thach Phan, Gwiy-Sang Chung, *Appl. Surf. Sci.* **257**, 3285 (2011).
- [8] M. B. Shahzad, Y. Qi, H. Lu, X. Wang, *Thin Solid Films* **534**, 242 (2013).
- [9] P. Bertrand, Y. De Puydt, J.-M. Beuken, P. Lutgen, G. Feyder, *Nucl. Instrum. Methods Phys. Res. Sect. B* **19-20**, 887 (1987).
- [10] E. Fortunato, M. H. Godinho, H. Santos, A. Marques, V. Assunção, *Thin Solid Films* **442**(1-2), 127 (2003).

- [11] Jianfeng Su, Qiang Niu, Chunjuan Tang, Yongsheng Zhang, Zhuxi Fu, *Optoelectron. Adv. Mat.* **5**(7), 751 (2011).
- [12] C. Nunes de Carvalho, G. Lavareda, E. Fortunato, H. Alves, *Mater. Sci. Eng. B* **118**(1-8), 66 (2005).
- [13] Z. L. Pei, X. B. Zhang, G. P. Zhang, J. Gong, C. H. Sun, R. F. Huang, *Thin Solid Films* **497**, 20 (2006).
- [14] B. Lin, Z. Fu, Y. Jia, *Appl. Phys. Lett.* **79**(7), 943 (2001).
- [15] Jianfeng Su, Changqing Wang, Chunjuan Tang, J. Alloy. *Compd.* **509**(20), 6102 (2011).
- [16] E. S. Shim, H. S. Kang, J. S. Kang, J. H. Kim, S. Y. Lee, *Appl. Surf. Sci.* **186**(1-4), 474 (2002).

*Corresponding author: sujianfengvy@163.com